NATIONAL BUREAU OF STANDARDS REPORT

NBS PROJECT 9120-12-91124

July 24, 1962

NBS REPORT 7286

A NEW METHOD OF TIME SIGNAL MODULATION AND DEMODULATION OF VLF CARRIERS

A. H. Morgan

U. S. DEPARTMENT OF COMMERCE

NATIONAL BUREAU OF STANDARDS

BOULDER LABORATORIES

Boulder, Colorado

IMPORTANT NOTICE

A NEW METHOD OF TIME SIGNAL MODULATION AND DEMODULATION OF VLF CARRIERS

A. H. Morgan

1. INTRODUCTION

With the recent demands for increased accuracy of clock synchronization and time interval measurements, due to the advancements in science and particularly in connection with the missile ranges and satellite tracking stations, it is evident that the present hf radio time services [Iijima, 1947; Morgan, 1959, and NBS, 1960] are in many cases inadequate. In view of the much more stable phase conditions at VLF, as reported by many workers [Pierce, 1957 and 1958; Crombie, 1958; Casselman, 1959; and Silkwood, 1959], along with its world-wide coverage [Watt and Plush, 1961] capabilities, it is of prime interest to develop means of distributing time signals via this medium. The limiting factors, however, are the narrow bandwidths available and the high Q's of the VLF antennas. These factors indicate that a new technique, instead of pulse modulation, must be used in order to distribute time in the VLF spectrum. A new modulation and demodulation method is described below.

2. OUTLINE OF THE METHOD FOR DISTRIBUTING TIME

Instead of modulating the VLF carrier at the transmitter with sharply rising pulses, two frequency-locked carrier signals, e_1 and e_2, with a spacing of $\Delta \omega$ radians/sec. as shown in figure 1, are alternately transmitted. One simple method of generating these signals is shown in figure 3.

Let the non-transient part of the transmitted signals be given as:

$$e_1 = \cos \omega_1 t \tag{1}$$

$$e_2 = \cos \omega_2 t \tag{2}$$

where t is the elapsed time from some initial known epoch on the time scale being distributed and ω_1 and ω_2 are frequencies in radians per unit time on the same time scale. Then under steady state conditions, the times, t_{T_n}, at the transmitter at which the two signals are in phase-opposition occurs when: (see Fig. 2a)

$$\omega_2 t_{T_n} - \omega_1 t_{T_n} = n\pi \qquad (n = \pm 1, \pm 3, \pm 5 \ldots) \tag{3}$$

or

$$t_{T_n} = \frac{n\pi}{\omega_2 - \omega_1} \tag{4}$$

The carrier signals ideally at the receiver will then be, respectively:

$$e_{r_1} = \cos \omega_1 (t - t_1) \tag{5}$$

and:

$$e_{r_2} = \cos \omega_2 (t - t_2) \tag{6}$$

These signals will be in phase-opposition at the receiver at times t_{R_n} (see Fig. 2b) given by:

$$\omega_2 (t_{R_n} - t_2) - \omega_1 (t_{R_n} - t_1) = n\pi \qquad (n = \pm 1, \pm 3, \pm 5 \ldots) \tag{7}$$

$$(\omega_2 - \omega_1)\, t_{R_n} = \pm n\pi + \omega_2 t_2 - \omega_1 t_1 \tag{8}$$

or when:

$$t_{R_n} = \frac{n\pi + \omega_2 t_2 - \omega_1 t_1}{\omega_2 - \omega_1} \tag{9}$$

At the receiver, the times at which the two signals are in phase-opposition will differ from the corresponding times at the transmitter. This time difference, t_d, may be obtained by subtracting (4) from (9), thus (Fig. 2):

$$t_d = (t_{T_n} - t_{R_n}) = \frac{\omega_2 t_2 - \omega_1 t_1}{\omega_2 - \omega_1} \tag{10}$$

An alternate form may be obtained by use of the relationship:

$$t = \frac{d}{v}$$

where t is the time delay of a radio signal which travels a distance d with a phase velocity v, thus:

$$t_d = \left[\frac{\omega_2 / v_2 - \omega_1 / v_1}{\omega_2 - \omega_1} \right] d \tag{11}$$

If the phase-velocities and distance are known, the times t_{R_n}, at which the two received carriers are in phase-opposition may then be determined quite precisely. To determine the occurrence time of a particular phase-opposition, approximate knowledge of this time must first be obtained either from observation of the switching sequence, as described in paragraph 3, or from some other source such as hf time signals. This information may be then used to identify a given crossover of ω_1 at the receiver with that as transmitted, thus giving "microsecond" resolution.

Each received carrier signal is used to phase-lock two, highly stable, locally derived signals of the same nominal frequency (see Fig. 17.) Since these signals are locally generated they may have very constant amplitude and low (noise) jitter.

This is an important consideration in the demodulation system. It should be emphasized here that the timing accuracy achieved with this method will be limited only by the transmission fluctuations of the VLF signals. This important aspect of the timing problem has been dealt with in detail in another paper [Watt, Plush, Brown and Morgan, 1961].

3. PROGRAMMING

In order to make the method of time distribution independent of other time signals, such as those from WWV, a suitable transmitting program may be established. For instance, one-second time markers may be achieved by switching from one carrier to the other at a one-second rate, while one-minute markers may be identified by omitting the switching for, say, five seconds every minute; hourly markers may be achieved by further changes in the switching program; etc. However, to make full use of this type of programming, special receiving circuits must be devised in order to detect the precise occurrence of each switching time.

4. TRANSMITTING ANTENNA SYSTEM

4.1 Switching from ω_1 to ω_2

To prevent large amplitude transients from occurring in the transmiting antenna system, when changing the transmitted frequency from ω_1 to ω_2, and vice versa, it may be necessary to reduce the output power of the transmitter to nearly zero. The antenna would then be automatically retuned to the other frequency, and then full power would be restored precisely at a zero crossover time of the frequency to be transmitted, in order to minimize the antenna transients.

4. 2 Antenna Retuning

The retuning of the antenna from series-resonance at ω_1 to ω_2 may be accomplished automatically by use of a circuit such as shown in figure 4. The comparison of the radiated phase of the signal being transmitted, with that as provided to the transmitter input, is made in a phase detector and the error signal used in a feedback system to control the antenna reactance. As shown in figure 5a, a saturable reactor consitutes a part of the antenna tuning reactance and this component is varied to retune the antenna.

5. PHASE STABILITY OF TRANSMITTING SYSTEM

5. 1 Phase Stability of Antenna System

A high-Q series resonant circuit, such as a VLF antenna, with an equivalent circuit as shown in figure 5 b, obviously has a large phase-shift vs. frequency characteristic. Therefore, any detuning of the antenna due to effects of wind, snow, ice, etc. may introduce undesirable phase-shift into the transmitted signals.

Experience has shown [Brown, 1960] that the fractional time stability of an antenna, in terms of the period of one cycle, depends mainly on the fractional antenna capacitance changes. The approximate relationship is:

$$\left(\frac{\delta t}{T}\right) \cong +\ 0.159 Q_0 \ (\Delta c/c) \qquad (12)$$

where $T = \left(\frac{2\pi}{\omega_1}\right)$, δt is the apparent time change caused by a fluctuation of the antenna capacitance, and Q_0 is the quality factor at resonance. This equation may also be rewritten to give the maximum capacitance change that can be tolerated if the fractional time jitter is not to exceed $\left(\frac{\delta t}{T}\right)$:

$$(\Delta c/c) \cong 6.3 d(\delta t/T) \qquad (13)$$

where $d = 1/Q_0$, is the dissipation factor of the antenna.

For example, if $Q_0 = 10^3$, $f = 20$ kc, $T = \frac{1}{f_1} = 50$ μsec., and a δt of 1 μsec. is desired, then $(\Delta c/c) \cong 1.4 \times 10^{-4}$. At 20 kc, using a value $c = 0.008$ μf for the antenna capacitance, Δc could not exceed about 2 picofarads. The phase-lock system shown in figure 7 would be used to correct for the phase change caused by the capacitance changes that may occur in the antenna system.

5.2 Phase Stability of the Transmitter

A. Single Carrier System

Another source of phase instability in the system is in the tuned circuits of the transmitter. An equivalent circuit is shown in figure 6, wherein the antenna load resistance is included in the resistance shown. It may be seen that fractional changes in the transmitter tank circuit components, C or L, may also be related to the fractional time stability by (12).

B. Dual Carrier System

In setting a remotely located clock to the transmitted time, it is of course necessary to establish a time (or phase) reference at the receiving location. This is accomplished by reference to the times, t_{R_n}, when the received carriers are at phase opposition and relating this to the times, t_{T_n}, at the transmitter when phase opposition occurred there, as previously described. By generating both carriers from the same source at the transmitter (see Fig. 3) and compensating for the phase variations (Fig. 7) in the transmitting system, the necessary stability of the zero crossovers of each carrier frequency, as transmitted, maybe achieved.

6. PROPAGATION OF VERY LOW FREQUENCY SIGNALS

6.1 Phase Velocity

It has been shown that the diurnal variation of the phase of VLF waves propagated over great distances is almost directly proportional to the path length which is in daylight [Wait, 1959]. A theoretical model which has been proposed [Crombie, Allan and Newman, 1958] and extended [Wait, Sept 1958, Dec 1958; Jean, 1957; Wait and Murphy, 1956; Wait, 1959] is a sharply bounded isotropic ionosphere which is concentric with the surface of the earth. The ionospheric reflection coefficient at highly oblique incidence is taken as nearly unity and with a phase near 180°.

At great distances (>3000 km) the higher order modes are sufficiently attenuated so that only the mode of order n = 1 need be considered. The phase velocity in such a waveguide can then be approximated by [Wait, 1959]:

$$v \cong c\left(1 - \frac{\lambda^2}{16h^2}\right)^{-1/2}\left(1 - \frac{h}{2a}\right) \cong c\left(1 - \frac{h}{2a} + \frac{\lambda^2}{32h^2} + \ldots\right) \quad (14)$$

Where: c = velocity of light in vacuo

h = height of reflecting layer

a = radius of the earth

λ = wavelength

Taking differentials, it is seen that:

$$\frac{\Delta v}{c} \cong - \left[\frac{h}{2a} + \frac{\lambda^2}{16h^2}\right] \frac{\Delta h}{h} \tag{15}$$

where Δv is a change in phase velocity resulting from a change of height Δh. Results of precise relative phase measurements [Pierce, 1957 and 1958; Allan, Crombie and Penton, 1956; Crombie, Allan and Newman, 1958] and an analysis of the data [Wait, 1959] indicate that at VLF, a mean value of h is of the order of 80 km, with a total diurnal change of about 16 km ± 2 km.

From equation (14) it is easy to see that the phase velocity is also a function of the wavelength, λ, which indicates that at VLF the propagation medium is dispersive.

At the present time the phase velocity of signals around 20 kc is not accurately known although at lower frequencies it has been determined with a fair degree of accuracy [Wait, 1961]. Before the system described here can be fully evaluated measurements of the phase velocity and dispersion around 20 kc must be made. This problem is discussed in another paper [Watt, Plush, Brown and Morgan, 1961].

7. RECEIVING SYSTEM DESIGN

7.1 Receiving System Requirements

In order to determine time with "microsecond" resolution:

(a) The system must be capable of detecting the condition of phase opposition of the two locally generated signals.

(b) The locally generated signals must be produced by a technique which allows one to know that they can be in phase opposition only at certain possible times so that one is left only with the problem of deciding which of the possible occurrence times is the actual occurrence time of a particular phase opposition.

(c) The possible occurrence times must be sufficiently separated that approximate knowledge of the occurrence time is sufficient to limit the set of possible occurrence times to only one member.

(d) A method of arriving at the approximate occurrence time must be provided. This might involve the switching times, described in paragraph 3, or it might involve other less precise time signals, such as those from WWV or WWVH.

This requires, as mentioned before, that the times, t_{R_n}, be identified with the times, t_{T_n}. This requires that the precise delay time, t_d, for each given path must be accurately determined.

7.2 Receiver Bandwidth Versus Phase (Time) Stability

It may be shown [Valley and Wallman, 1948] that in a synchronous, single-tuned, amplifier with an equivalent circuit of a single-tuned stage as shown in figure 8, that the overall radian bandwidth $\left(\omega_{B_n}\right)$ of n identical stages, is given to a good approximation as:

$$\omega_{B_n} \cong \left(\frac{\omega_B}{1.2\sqrt{n}} \right) \tag{16}$$

where:

$$\omega_B = \left(\frac{1}{RC} \right) = \frac{\omega_0}{Q_0} \tag{17}$$

ω_B is defined as the radian bandwidth of a single receiver stage, Q_0 is the quality factor of the R, L, C circuit and ω_0 is the resonant angular frequency. Putting (17) in (16) gives the approximate overall bandwidth of n cascaded stages as:

$$\omega_{B_n} = \left(\frac{\omega_0}{1.2\sqrt{n}\, Q_0}\right) \tag{18}$$

The phase deviations in each stage, due to component instability, may be assumed to be random and independent if the changes are not due to a common precipitating fluctuation of a parameter such as temperature, so that the overall rms phase change, $\Delta\theta_n$, in n independently fluctuating stages, in terms of the angle stage rms fluctuations of a single stage is:

$$\Delta\theta_n = (\sqrt{n}\, \Delta\theta) \tag{19}$$

The overall fractional time change due to a small capacitance change in a single stage is from (13), (18) and (19):

$$\left(\frac{\delta t}{T}\right) \cong \frac{0.159\sqrt{n}\,\omega_0}{\omega_B} \left(\frac{\Delta c}{c}\right) \tag{20}$$

The minimum radian bandwidth, ω_B, of a single stage that may be used without degrading the overall fractional time stability, $\left(\frac{\delta t}{T}\right)_n$, for a given capacitance change per stage, is:

$$\omega_B \cong \frac{0.159\sqrt{n}\,\omega_0}{\left(\frac{\delta t}{T}\right)} \left(\frac{\Delta c}{c}\right) \tag{21}$$

For example, a TRF receiver has n = 4 stages, $\left(\frac{\Delta c}{c}\right) = 10^{-3}$, and the overall fractional time stability, $\left(\frac{\delta t}{T}\right)$, must be at least 0.02. Also, $\left(\frac{\omega_0}{2\pi}\right) = 20$ kc. What may be the minimum bandwidth of each stage ? The minimum overall bandwidth?

$$f_{b_{min}} = \left(\frac{\omega_B}{2\pi}\right) = \frac{0.159 \times \sqrt{2} \times 2 \times 10^4 \times 2\pi}{0.02 \times 2\pi} \times 10^3 = (318c/s)$$

The minimum overall bandwidth, $f_{B_n} = \left(\frac{\omega_B}{2\pi}\right) = (133c/s)$.

7.3 Signal-to-Noise at Receiver

It may be shown [Watt and Plush, 1959] that the precision of an integrated frequency measurement, using a phase comparison method, is given approximately by:

$$\varepsilon \cong \frac{N/C}{\omega T^{3/2} B_n^{1/2}} \qquad (22)$$

Where: C and N are rms carrier and noise voltages, B_n is the predetection bandwidth, ω is the radian frequency and T is the integration time. In this system, the VLF receiver (Fig. 9) is designed so that each carrier frequency received is alternately phase compared with a local signal of the same nominal frequency and the error voltage is used to correct the phase of each of the local reference signals. Thus equation (22) is valid and, by rewriting it, the required carrier-to-noise ratio may be determined for a desired precision of frequency comparision:

$$C/N \cong \left(\frac{1}{\varepsilon \omega T^{3/2} B_n^{1/2}}\right) \qquad (23)$$

8. PHASE-LOCK SYSTEM IN RECEIVER

8.1 General Description

In figure 9 a single-carrier phase-lock system is shown in simplified form that has proved very accurate and reliable [Looney, 1961; Morgan and Andrews, 1961]. The local reference frequency, nominally the same as that received, is derived from the local oscillator. It is important that the latter be as free as possible of phase perturbations.

The local reference frequency, after passing through the phase-shifter, is kept phase-locked to the received reference frequency by the action of the phase-detector and servosystem as shown in the block diagram.

To convert the angular position of the phase-shifter to a voltage (or current), for monitoring purposes, a 360° potentiometer is connected to its shaft. With a constant direct voltage applied across the linear potentiometer, the position of the shaft then is proportional to the voltage appearing between the movable tap and one side of the potentiometer. The latter voltage (or current) is recorded versus time of day on a strip chart. Although in figure 9 the phase-shifter is used at the nominal received frequency, it may be actually used at a higher frequency in, or ahead of, the frequency synthesizer.

8.2 Analysis of a Phase-Lock System

In figure 10 is shown a block diagram of the phase-lock system for a single carrier. If the phase-detector operation is limited to its linear range, and with the input signals given as:

$$\varepsilon_1 = A \sin\left(\omega_1 t + \theta_1(t)\right) \qquad (24)$$

and

$$\varepsilon_2 = A \cos \left[\omega_2 t + \theta_2 (t) \right] \tag{25}$$

the filtered output of the phase detector may be shown to be, approximately:

$$\varepsilon_0 \cong \frac{A^2 K_1}{2} (\Delta \theta) \tag{26}$$

where $\Delta \theta = \left[\theta_1 (t) - \theta_2 (t) \right]$ and K_1 is a characteristic of the phase-detector.

The system may then be regarded as a linear servosystem as shown in figure 10, with ω_i (S) as the input signal and ω_0 (S) as the output signal. The factor 1/S takes into account the integration of frequency-difference to phase-difference [McAleer, 1959] in the phase-detector, F(S) is the transfer function of the low-pass filter, and K_2 / N is the gain of the rest of the system, consisting of the combination of the gains of the amplifier, K_a, servomotor, K_m, the phase-shifter, K_ϕ, and gear-train reduction ratio, N.

Writing the equation in the terms of the complex variable S in transfer function form yields:

$$G(S) = \frac{\omega_0 (S)}{\Delta \theta (S)} = \frac{A^2 K_1 K_2}{2N} \frac{F(S)}{S} = K_3 \frac{F(S)}{S} \tag{27}$$

It is then possible to write the closed-loop transfer function, letting $K_3 \equiv \left(\frac{A^2 K_1 K_2}{2N} \right)$, as:

$$Y(S) = \frac{\omega_0(S)}{\omega_i(S)} = \frac{G(S)}{1+G(S)} = \frac{K_3 \frac{F(S)}{S}}{1+K_3 \frac{F(S)}{S}} = \frac{K_3 F(S)}{S+K_3 F(S)} \tag{28}$$

Now the transfer function, F(S), of the RC filter (Fig. 12) in terms of S may be shown to be:

$$F(S) = \left(\frac{\varepsilon_0}{\varepsilon_i}\right) = \left(\frac{1/T_1}{S+1/T_1}\right), \text{ where } T_1 = RC \tag{29}$$

Using this in (29), it may be rewritten as (see Fig. 11):

$$Y(S) = \frac{\omega_0(S)}{\omega_i(S)} = \frac{K_3/T_1}{S(S+1/T_1) + K_3/T_1} = \frac{K_0}{S^2 + S/T_1 + K_0} \tag{30}$$

where: $K_0 = K_3/T_1$.

The denominator of (30) is of the form:

$$S^2 + 2\,\xi\,\omega_n S + \omega_n^2 \tag{31}$$

where:

$$\xi = \left(\frac{1}{2\omega_n T_1}\right) = (F/F_c) \tag{32}$$

the ratio of actual damping to critical damping, and:

$$\omega_n = \sqrt{K_0}, \text{ is} \tag{33}$$

the natural (undamped)frequency of the system. The roots of (31) are, of course, the poles of (30) and are:

$$S_1 = -\omega_n \xi + j\omega_n \sqrt{1-\xi^2} = -a + j\omega_d \tag{34}$$

$$S_2 = \omega_n \xi - j\omega_n \sqrt{1-\xi^2} = -a - j\omega_d \tag{35}$$

where:

$\alpha = \omega_n \xi$, and $\omega_d = \omega_n \sqrt{1-\xi^2}$, the damped frequency.

The closed loop transfer function (30) may be written in terms of its poles as:

$$Y(S) = \frac{\omega_0(S)}{\omega_i(S)} = \frac{K_0}{(S-S_1)(S-S_2)} \tag{36}$$

This is the transfer function of a position control servosystem [D'Azzo and Houpis, 1960].

Two important characteristics of the servosystem are evident from the above. One is that it may never become unstable regardless of the value of the gain, K_0, as further shown in the root-locus plot, figure 13.

The second characteristic of this system is that, unlike a frequency-lock system, the phase-lock servo requires [McAleer, 1959] no steady-state error in the controlled variable (ω), but instead uses an error in its integral (θ). Therefore, the average controlled frequency is identical to that of the received reference frequency. The effects of noise in the received reference frequency will be discussed in paragraph 8.4.

8.3 System Bandwidth

The response of a servosystem to random noise on the input can be expressed in terms of its noise bandwidth [McAleer, 1959], which is:

$$F_n = \frac{\pi\omega_n}{4\xi} \left[1+\left(2\xi - \frac{\omega_n}{K_3}\right)^2\right] \tag{37}$$

For minimum noise bandwidth the following conditions [Rey, 1960] must be satisfied:

$$\xi_{opt} = \tfrac{1}{2}\sqrt{1 + \left(\frac{\omega_n}{K_3}\right)^2} \tag{38}$$

It can also be shown that the 6 db bandwidth [D'Azzo and Houpis, 1960], ω_b, of a position control servosystem is given by:

$$\omega_b = \left[1-2\xi^2 + \left\{ 1 + (1-2\xi^2)^2 \right\}^{\frac{1}{2}} \right]^{\frac{1}{2}} \omega_n \tag{39}$$

and that for $\xi = 0.7$, $\omega_b = \omega_n$, where ω_n is the natural radian frequency of the system.

From (39) it may be seen that the larger the damping ratio, ξ, the smaller the radian bandwidth, ω_b. Using some relationships given above, i.e., that $K_3 \equiv \dfrac{A^2 K_1 K_2}{2N}$ and that $K_0 \equiv K_3/T_1$, and from (32) and (34) it may be seen that:

$$\xi = \frac{1}{2\omega_n T_1} = \frac{1}{2\sqrt{K}\ T_1} = \frac{\sqrt{2N}}{2A\sqrt{K_1 K_2 T_1}} = K N^{1/2} \tag{40}$$

Where $K \equiv \dfrac{\sqrt{2}}{2A\sqrt{K_1 K_2 T_1}}$

Since ξ is proportional to $N^{1/2}$, the gear-reduction ratio, an increase in N will result in a narrower radian bandwidth, ω_b. It is easy to achieve bandwidths in phase-lock servosystems of the order of 0.001 c/s.

8.4 Perturbations by Noise on Received Reference Frequency

The above shows that a servosystem may be regarded as a lowpass filter on the received refernece signal but with a controllable bandwidth. That is, it has a limited speed of response and responds only to those received noise components that fall within its effective bandwidth.

Following Watt and Plush [Watt and Plush, 1961], if the received reference frequency to the servosystem is contaminated by a small amount of narrow band noise, the maximum phase variation of the resultant is $\phi_m = n/c$, where n and c are the peak noise and carrier values. If the standard deviation of phase, σ_ϕ, is desired, replace n with N and c with $\sqrt{2}C$ to obtain:

$$\sigma_\phi \cong \frac{N}{\sqrt{2}C} \tag{41}$$

where C and N are rms carrier and noise voltages.

If this signal is compared in a phase-detector with an unperturbed signal such that there are r cycles of this signal present, and the total fractional phase jitter (since ϕ is normally distributed)is $\sqrt{2}\sigma_\phi$, then the output of the phase detector is:

$$\varepsilon = \left(\frac{\sqrt{2}\sigma_\phi}{\phi}\right) = \frac{\sqrt{2}\sigma_\phi}{2\pi r} \tag{42}$$

Using (42) in (41):

$$\left(\frac{\sigma_\phi}{\phi}\right) \cong \frac{N/C}{\sqrt{2}\ 2\pi r} \tag{43}$$

Now, in a servosystem the received reference signal is integrated over a period, T, and it is passed through a pre-detector filter of bandwidth B. Thus a reduction is obtained in the phase jitter of approximately $(T\ B)^{-\frac{1}{2}}$. Also, it is observed that the integration time is $T = \frac{2\pi}{F_n}$, where F_n is the servo bandwidth in radians, and T is in seconds, so that the fractional phase jitter in the servosystem now becomes:

$$\left(\frac{\sigma_\phi}{\phi}\right) \cong \frac{N/C}{2\pi f_1 T^{3/2}\left(\omega_B\right)^{1/2}} = \frac{(N/C)\, F_n^{3/2}}{(2\pi)^{3/2}\, \omega_1 \left(\omega_B\right)^{1/2}} \qquad (44)$$

where the predetection bandwidth is now given in radians, or $\omega_B = 2\pi B$, $r = fT$ and ω_1 is the radian frequency of the reference signal.

Thus, the phase-jitter or fluctuations may be reduced by making: (a) servo bandwidth, F_n, smaller; (b) reference frequency, ω_1, larger, (although this is fixed in a given system); or, (c) N/C smaller.

For example, if $\omega_1 = 2\pi \times 20$ kc, $N/C = 10^{-2}$, $\omega_B = 2\pi \times 10^2$, and $F_n = 2\pi \times 10^{-3}$, then:

$$\left(\frac{\sigma_\phi}{\phi}\right) \cong 2.5 \times 10^{-11}.$$

9. DETECTION OF TIMES OF OCCURRENCE t_{R_n}, OF PHASE-OPPOSITIONS AT RECEIVER

9.1 Pulse Sharpener Circuit

In order to determine the antiphase times, t_{R_n}, of the two received carriers, the signals are amplitude limited and the resulting square waves are differentiated to produce sharp pulses. To further sharpen them, a circuit such as shown in figure 14a may be used [Reiffel, 1951]. It is shown that the peak voltage of the sharpened output pulse, v_p, is given in terms of its width, σ, and the width of the input pulse, γ, as (see Fig. 14b):

$$v_p = v'_p \left[\frac{\sigma}{\pi\gamma} \right] \quad (45)$$

where, $v'_p = (I\frac{\gamma}{c})$, I is input peak pulse current, and c is capacitance.

Solving (45) for σ:

$$\sigma = \left(\frac{v_p}{v'_p} \right) \pi\gamma \quad (46)$$

For instance, if $\left(\frac{v_p}{v'_p} \right) = 0.01, \gamma = 3 \times 10^{-5}$ sec., then

$\sigma = 0.03\, \pi\, 10^{-5} \cong 10^{-6}$ sec.

9.2 Pulse Coincidence Circuit

The active pulse coincidence circuit [Lewis and Wells, 1959], shown in figure 15, is designed to take pulses of equal amplitude, equal width and the same polarity (inputs A and B) and indicate when pulse A is coincident with pulse B. An output pulse indicates coincidence; this pulse is further amplified to increase the sensitivity of the circuit.

In figure 16 are shown the waveforms of the two signals, ω_1 and ω_2. Also shown is that the same polarity pulses of ω_1 are spaced by a time interval, $T_1 = \frac{2\pi}{\omega_1}$, while those of ω_2 are spaced $T_2 = \frac{2\pi}{\omega_2}$. Thus, the difference between the periods, is given by $\Delta T = (T_2 - T_1) =$

$$\left(\frac{2\pi}{\omega_2} - \frac{2\pi}{\omega_1} \right)$$

10. TIME DEMODULATION RECEIVER SYSTEM

10.1 General Requirements

The remaining factors that must be included in the receiving system in order to achieve "microsecond" timing and clock setting are to:

(a) provide " memories" in the dual-carrier receiver so as to store information regarding the phase of one carrier during the time the other is being received, and vice versa

(b) provide means of compensating for any phase delays of each carrier in the receiving system

(c) provide means of identifying a given cycle of the "main" carrier with that as transmitted

(d) provide automatic means for accurately reading out the received time on demand.

Other desirable features which are optional but would enhance the usefulness of the receiving system would be to:

(a) provide for automatic steering of a "microsecond" clock connected to the receiver

(b) provide for automatic setting of a "microsecond" clock connected to the receiver

(c) fail-safe circuitry and an indication when the clock is incorrect.

10.2 A Possible Dual-Carrier Receiver Design

In figure 17 is a possible design for dual-carrier time receiver (with the required "memories" not shown) to utilize alternate reception of the two carriers. As may be seen, it consists of two phase-lock systems interconnected so that the "main" carrier controls the output phase of the reference oscillator frequency, ω_1, and the "sideband" carrier then controls the phase of the reference "sideband" frequency, ω_2. The rate generators control the angular frequency of the phase shifters so that:

(a) They will always keep their respective reference signals phase-locked to the received signals

(b) They will continue to run at the last corrected rate when the alternate carrier is being received; thus they constitute the "memory" devices mentioned above that are required because the two carriers are alternately transmitted

(c) they will continue to run at the last corrected rate when both of the carriers transmissions are interrupted. This will permit the clock to free run at a rate which varies only because of the aging rate of the high quality local oscillator. When the transmissions are resumed, the accumulated time errors may be less than they otherwise would be and therefore the clock may be corrected in a much shorter time

10.3 Clock System Design

A. Pulse Generators

With the two reference signals, ω'_1 and ω'_2, phase-locked to the received carrier frequencies, ω_1 and ω_2, it is then possible to use signals of constant amplitude and low phase jitter in the clock system. (Diurnal phase shifts may be compensated for and this will be discussed in a later paragraph. In what follows here, it will be assumed that the diurnal effects have been minimized.)

The phase lock signals, ω'_1 and ω'_2, are squared by limiting, differentiated and then sharpened (see Fig. 16). Pulses from the sideband carrier are then reversed in phase (180^o) and both sets of pulses fed to a coincidence detector circuit. The above permits determining when the two received signals are in phase-opposition. The pulse generated by the coincidence of the pulses (ω'_1 and ω'_2) is then used to operate a gating circuit, which allows a pulse of ω'_1 (main carrier) to pass through it to the pulse divider circuit and thence to the clock.

B. Pulse Divider Circuit and Gate

The pulses, passed by the gating circuit, are phase-locked to the main carrier, ω_1, and thus each of the particular cycles used to mark the times t_{R_n}, of antiphase at the transmitter will be identified if:

(a) the gating circuit opens when the received signals are in antiphase; (b) the propagation delay time, t_d, of the signals from the transmitter to the receiver is accurately known; (c) the phase delays are compensated for in the receiving system.

Because the gate will pass pulses at a rate, $R = \Delta\omega / 2\pi$, c/s where $\Delta\omega = (\omega_2 - \omega_1)$, a divider circuit is used to permit choosing a lower rate, R′, which may be, say, 1c/s. These pulses then are used to interrogate or readout the clock once per second to determine if the system is working properly.

C. Clock Pulses

As shown in figure 17, the digital clock is driven by 1 mc/s pulses derived from the main carrier, thus permitting time to be accumulated in 1 μsecond increments. Therefore, the clock is also capable of reading out time with the same resolution. These pulses may be retarded (or advanced) in phase, initially, to compensate for the delays in the system. The propagation delay time must, of course, be accurately known also before this may be done.

D. Digital Clock

The clock shown in figure 17 is designed so that it may be read out at any time on demand without causing it to lose counts. A clock of an entirely different design [Hefley, 1960], but capable of readout on demand and using magnetic beam switching tubes, has been successfully used at National Bureau of Standards Boulder Laboratories.

11. CLOCK TIME AT RECEIVER

11.1 Clock Setting

Although it is relatively easy to control the rate of a clock using VLF radio signals, it is more difficult to accurately set a remote clock to agree with the one at the transmitter. At hf, where bandwidth is not a limitation, this is accomplished by transmitting rather short pulses whose leading edges are steep. At VLF this is not possible, as mentioned before. In this system the time reference at the receiver is established as described in paragraph 7.1 above.

11.2 Diurnal Effects

At VLF the diurnal changes in the reception time of the phase of the signals is quite large (20 to 70 μsec). It is of interest to determine what effect this might have on the readout time of the remote clock. There are two factors to be investigated that may cause the diurnal changes to affect the clock reading. One is the spacing, $\Delta\omega$, of the two carrier signals and the other is the change of height of reflection, Δh.

A. Effect of Carrier Spacing, $\Delta\omega$

Refer to equation (14), above, which is an approximate expression for the phase velocity of VLF waves at distances over 3000 km, in terms of a waveguide of mean height h. Now:

$$\left(\omega_2 t_2 - \omega_1 t_1 \right) = d \left(\frac{\omega_2}{v_2} - \frac{\omega_1}{v_1} \right) \tag{47}$$

where v is the phase velocity of the wave. If equation (14) is put into equation (47) the result is:

$$\left(\omega_2 t_2 - \omega_1 t_1 \right) \cong 2\pi\, d/c \left[(1 - h/2a)^{-1} \left(f_2 - f_1 \right) \left(1 + \frac{c^2}{32 h^2 f_1 f_2} \right) \right] \tag{48}$$

Using this result in equation (9) gives for the occurrence times, t_{R_n}:

$$t_{R_n} \cong \frac{n\pi + 2\pi\, d/c \left[\left(1 - h/2a \right)^{-1} \left(1 + \frac{c^2}{32 h^2 f_1 f_2} \right) \right]}{2\pi} \tag{49}$$

This may be further simplified by use of the binomial theorem:

$$t_{R_n} \cong \frac{n}{2} + d/c \left[1 + h/2a + \frac{c^2}{32 h^2 f_1 f_2} + \text{small order terms} \right] \tag{50}$$

This shows that, to the first order, the occurrence times, t_{R_n}, are independent of the spacing of the carriers, $\Delta f = \left(f_2 - f_1 \right)$.

B. Effect of Diurnal Changes of h on t_{R_n}.

If equation (50) is differentiated with respect to the height of reflection, h, and the small order terms neglected, the result is:

$$\delta t_{R_n} \cong d/c \left[\frac{1}{2a} - \frac{c^2}{16 f_1 f_2 h^3} \right] \delta h \tag{51}$$

If we let $d/c = t$, the propagation time of an electromagnetic wave in free space over a path length, d, then equation (51) may be written as:

$$\frac{\delta t_{R_n}}{t} \cong \left[\frac{1}{2a} - \frac{\lambda_1 \lambda_2}{16h^2} \right] \frac{\delta h}{h} \tag{52}$$

where $\lambda_1 = \frac{c}{f_1}$ and $\lambda_2 = \frac{c}{f_2}$. This gives the variations of the occurrence times, t_{R_n}, in terms of the "ideal" phase propagation time t, of the wave over a path of length d, due to variations in height, h.

Wait's result for the fractional time variation as received, of the phase of a single carrier at 16 kc [Wait, 1959, eq. 4] due to variations in h, is:

$$\frac{\Delta t}{t} \cong - [0.0097] \frac{\delta h}{h} \tag{53}$$

Using typical values in (52) for this system:

$h = 80$ km $\qquad \lambda_2 = 14.25$ km (21kc)
$\lambda_1 = 15$ km (20 kc)

we get:

$$\frac{\delta t_{R_n}}{t} \cong - [2.07 \times 10^{-3}] \quad \frac{\delta h}{h} \tag{54}$$

Thus, it appears that the occurrences times, t_{R_n}, suffer less diurnal change than the phase shift, Δt, of a single VLF carrier, both relative to the "ideal" phase propagation time, t.

C. Diurnal Compensation System

The system in figure 18 is designed to record continuously the received diurnal phase changes with reference to a highly stable local oscillator.

This information is later recovered from the recording and used to control a phase-locked servo not shown that subtracts the recorded phase-shift from the received signal. Under ideal conditions the two phase-shifts may essentially cancel [Fey, 1961] thus providing a VLF signal at the receiver substantially free of the diurnal phase changes. Although the frequency changes of the reference oscillator due to aging effects will be recorded along with the diurnal phase changes, it will not be serious under many conditions. For instance, if the diurnal shift is of the order of 50 μsec and the daily aging rate of the oscillator is 3×10^{-11} (3 μsec), then an elapsed time of several days between the recording and its subsequent use would generally be satisfactory.

Acknowledgment

Many helpful discussions were held with A. D. Watt, D. H. Andrews, and W. W. Brown. Also, many suggestions for improving the text by W. R. Atkinson are gratefully acknowledged.

12. REFERENCES

Allan, A. H., D. D. Crombie, and Q. A. Penton, Frequency variations in New Zealand of 16 kc/s transmissions from G B R Rugby, Nature, 177, 178-179 (Jan. 28, 1956).

Brown, W. W., Private communication (1960).

Casselman, C. J., D. P. Heritage, and M. L. Tibbals, VLF propagation measurements for the radux-omega navigation system, Proc. IRE, 47, No. 5, 829-839 (May 1959).

D'Azzo, J. J., and C. H. Houpis, Feedback control system analysis and synthesis (Book, McGraw-Hill Book Co., Inc., New York, N. Y., 1960).

Crombie, D. D., A. H. Allan, and M. Newman, Phase variations of 16 kc/s transmissions from Rugby as received in New Zealand, The Institution of Electrical Engineers, Proc. Pt. B. 105, 301-304 (May 1958).

Fey, R. L., Private communication (1961)

Hefley, G., Private communication (1960).

Iijima, Shigetake, and Gors Shibutani, Travel time of radio signals between Hawaii and Tokyo, Tokyo Astronomical Bulletin, Second Series No. 97, 1033-1050 (June 20, 1947).

Jean, A. G., Spherics, Proc. 12th URSI General Assembly, Boulder, Colorado, Pt IV, 1-50 (Sept. 1957).

Kay, Z., A new type of high speed coincidence circuit, Review of Scientific Instruments, 397 (June 1951).

Lewis, I. A. D., and F. H. Wells, Millimicrosecond pulse techniques, 137 Book (1959).

Looney, C. H. Jr., A VLF synchronizing system, Proc. IRE, 49, 448-452 (Feb. 1961).

McAleer, H. T., A new look at the phased-locked oscillator, Proc. IRE 47, 1137-1143 (June 1959).

Morgan, A. H., Precise time synchronization of widely separated clocks, NBS Technical Note No. 22 (July 1959).

Morgan, A. H. and D. H. Andrews, Methods and techniques of low and very low frequency monitoring at Boulder Laboratories, second conference of the consultative committee for the definition of the second, Sevres, April 1961, Document S-24.

NBS Miscellaneous Publication 236, Standard frequencies and time signals from WWV and WWVH (July 1, 1961).

Pierce, J. A., Intercontinental frequency comparison by very low-frequency radio transmissions, Proc. IRE 45, 794-803 (June 1957).

Pierce, J. A., Recent long-distance frequency comparisons, IRE Transactions on Instrumentation, 1-7, No. 3-4, 207-210 (Dec. 1958).

Reiffel, Leonard, Passive pulse sharpening circuits, Review of Scientific Instruments, 214 (March 1951).

Rey, T. J., Automatic phase control: theory and design, Proc, IRE 48, No. 7, 1760-1771 (Oct.1960).

Silkwood, J. A., Phase stability measurements of 18.6-kc radio transmissions, NEL Report, 899 (June 4, 1959).

Valley, G. E., and H. Wallman, Vacuum tube amplifiers 173 (McGraw-Hill Book Co., New York, N. Y. 1948).

Victor, W. K., The evaluation of phase stable oscillators for coherent communication system, Proc. of the 10th Annual symposium on frequency control, U.S. Signal Corps, (May 1956).

Wait, J. R., and K. Spies, A note on the phase velocity of VLF radio waves, J. Geophys, Res., 66, No. 3, 992-993 (March 1961).

Wait, J. R., Diurnal change of ionospheric heights deduced from phase velocity measurements at VLF, Letter to Editor of IRE, (May 1959).

Wait, J. R., and A. Murphy, Multiple reflections between the earth and the ionosphere in VLF propagation, Geofisica Pura e Applicata, 35, 61-72 (1956).

Wait, J. R., Propagation of VLF pulses to great distances, J. Research NBS, 61, 187-203 (Sept. 1958).

Wait, J. R., Transmission loss curves for VLF propagation, IRE CS6, (Transactions on communication systems), 58-61, (Dec. 1958).

Watt, A. D., and R. W. Plush, Power requirements and choice of an optimum frequency for a worldwide standard-frequency broadcasting station, J. Research NBS 63D, No. 1, 35-43 (Aug. 1959).

Watt, A. D., R. W. Plush, W. W. Brown, and A. H. Morgan, Worldwide standard frequency and time signal broadcasting, J. Research, Sec. D. (Nov.-Dec. 1961).

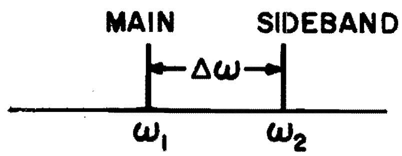

FREQUENCY SPECTRA

Fig. 1 – VLF SIGNALS

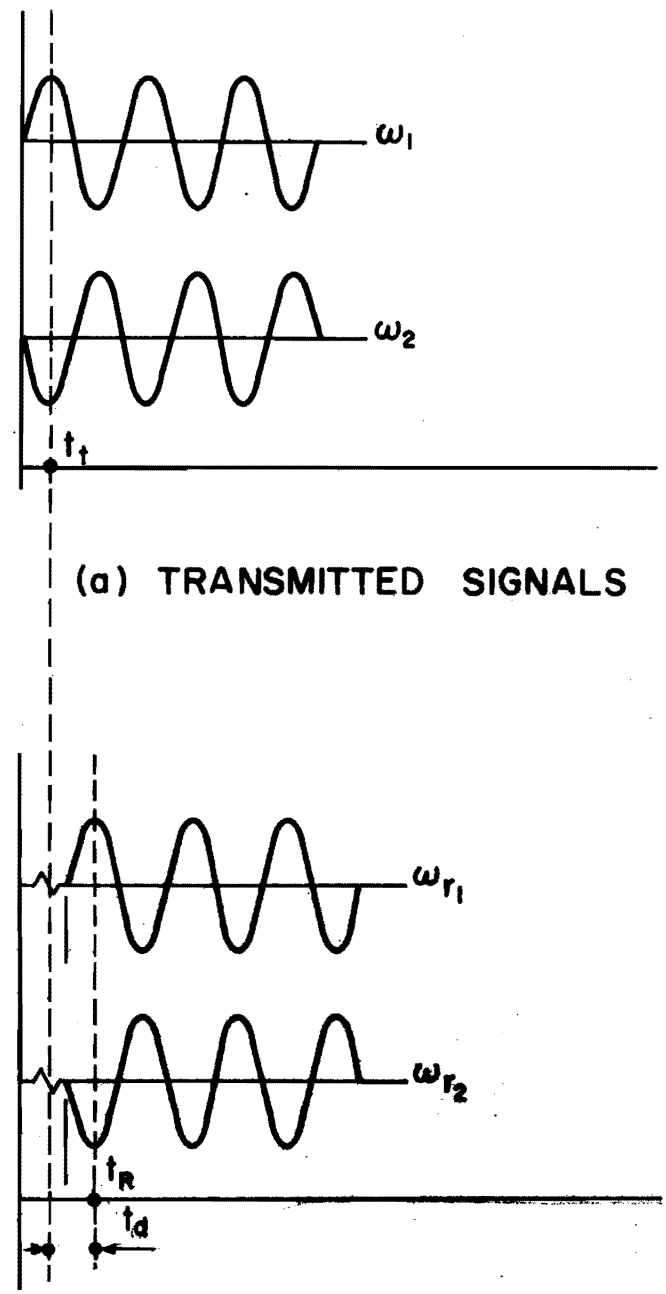

(a) TRANSMITTED SIGNALS

(b) RECEIVED SIGNALS

Fig. 2 – TRANSMITTED AND RECEIVED SIGNALS

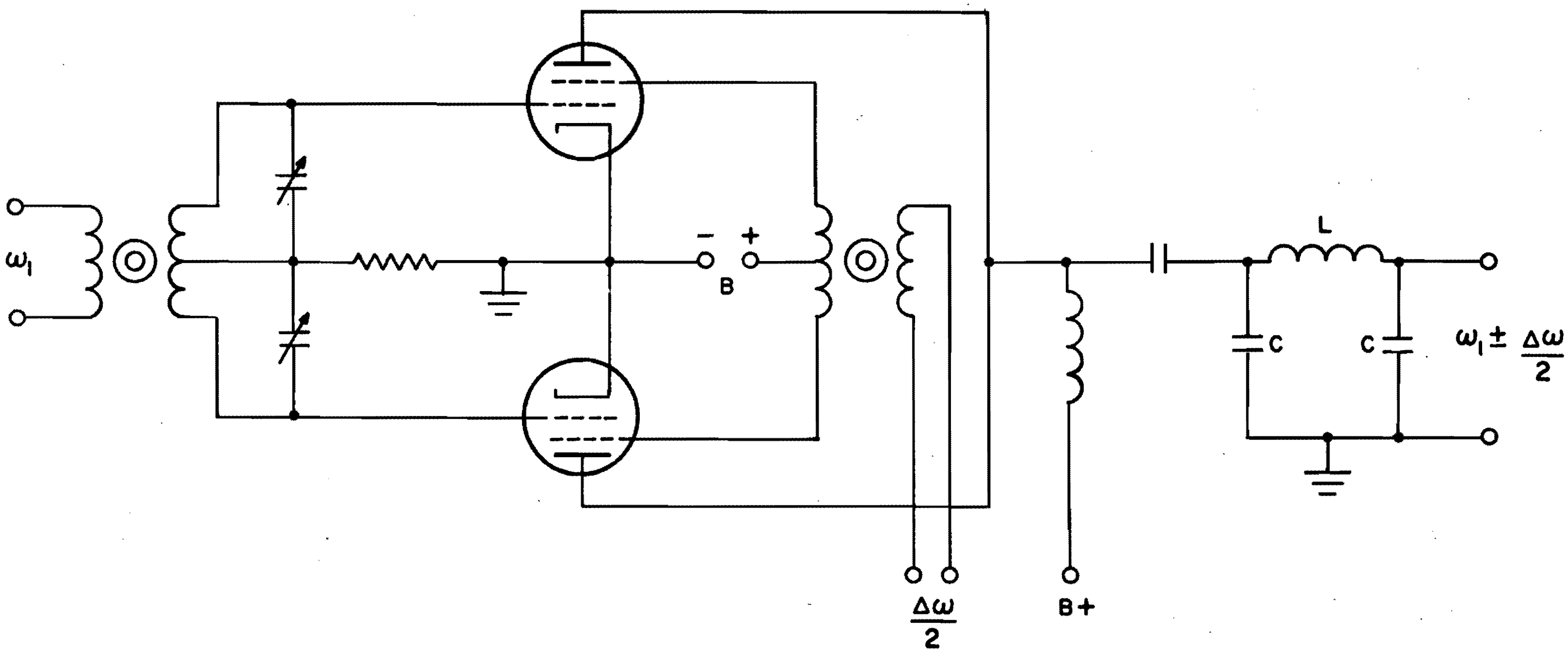

Fig. 3 ONE METHOD OF GENERATING DUAL-CARRIER SIGNALS

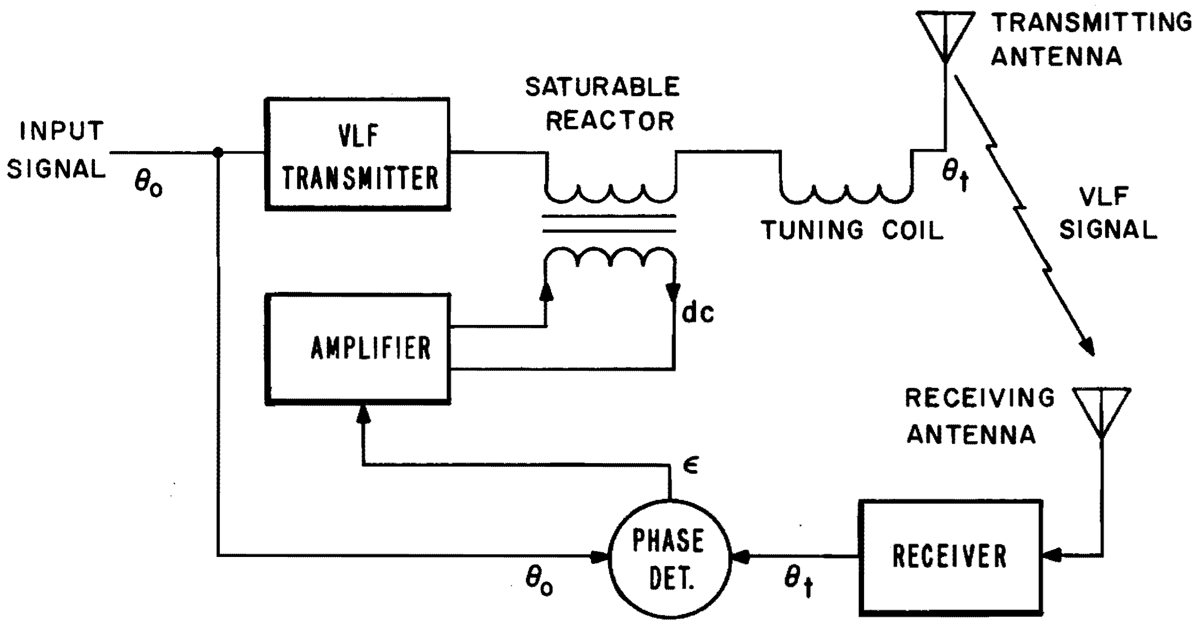

FIG. 4 AUTOMATIC TUNING CIRCUIT FOR ANTENNA

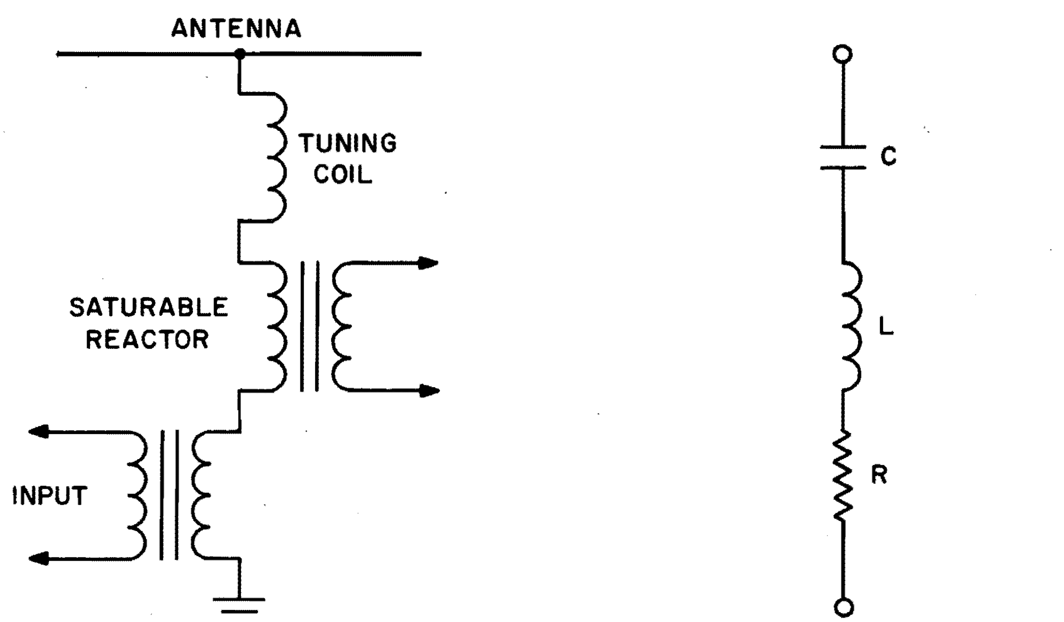

(a) ANTENNA SYSTEM (b) EQUIVALENT CIRCUIT

FIG. 5 VLF ANTENNA

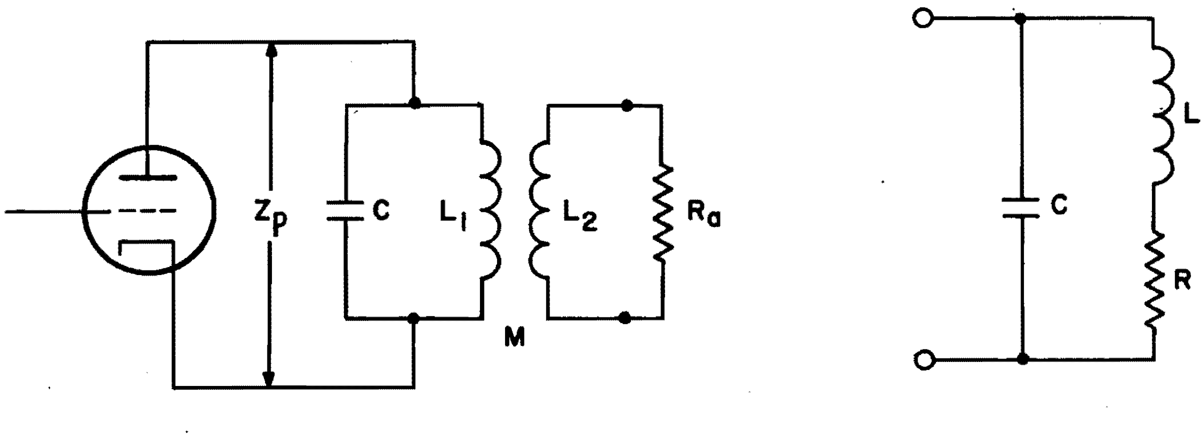

(a) CIRCUIT (b) EQUIVALENT CIRCUIT

FIG. 6 TRANSMITTER TANK CIRCUIT

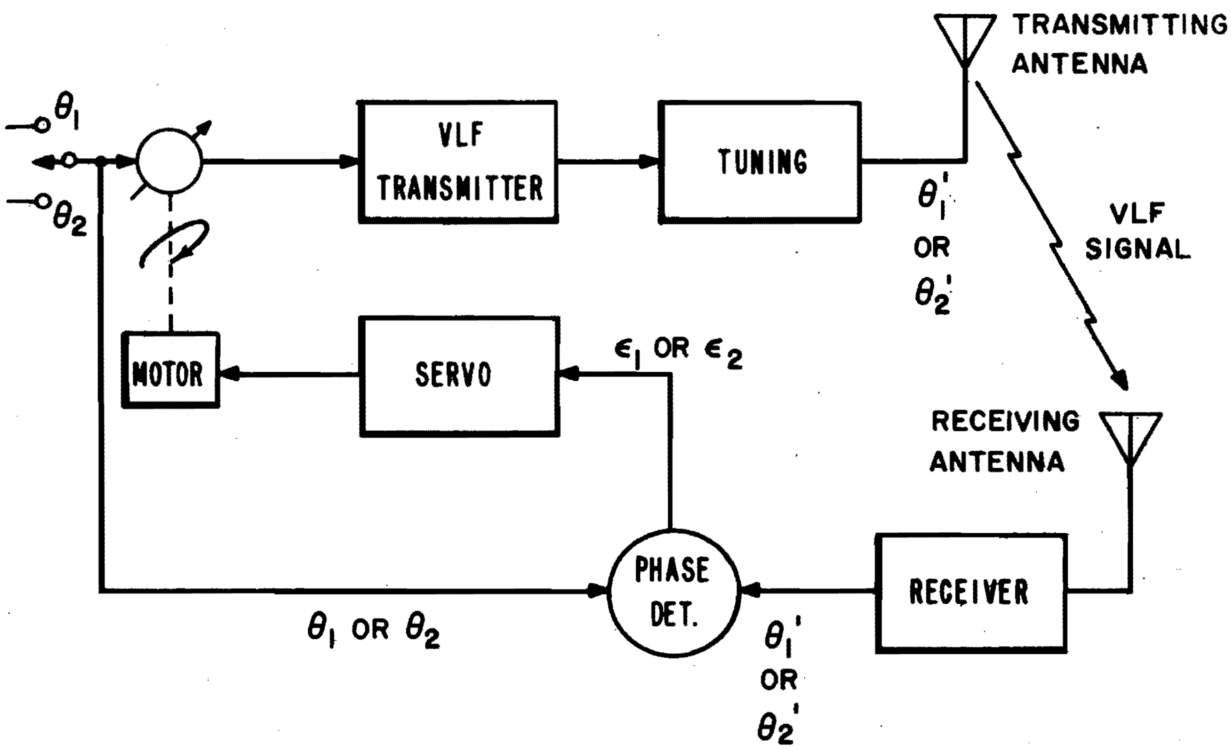

FIG. 7 TRANSMITTER AND ANTENNA AUTOMATIC PHASE CORRECTION SYSTEM

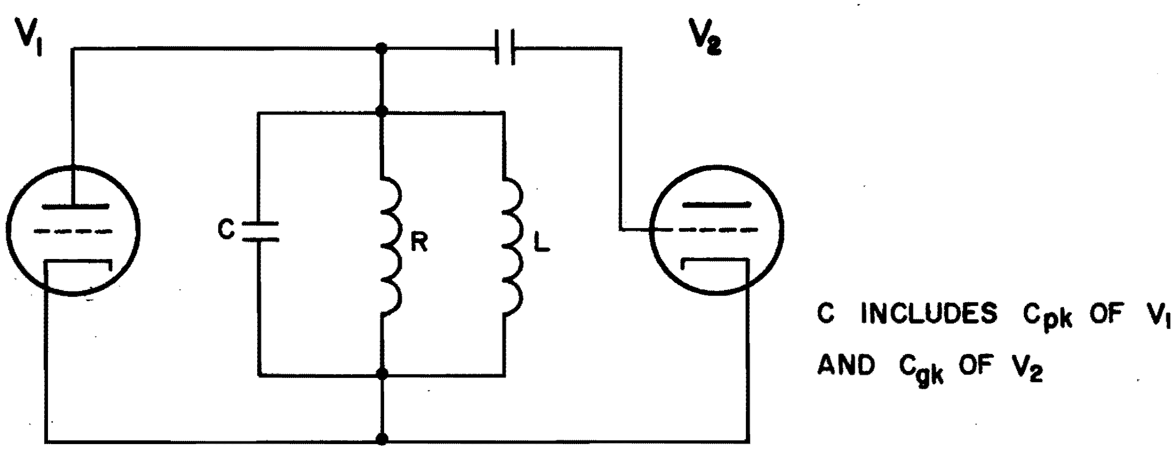

Fig. 8 RECEIVER TUNED CIRCUIT

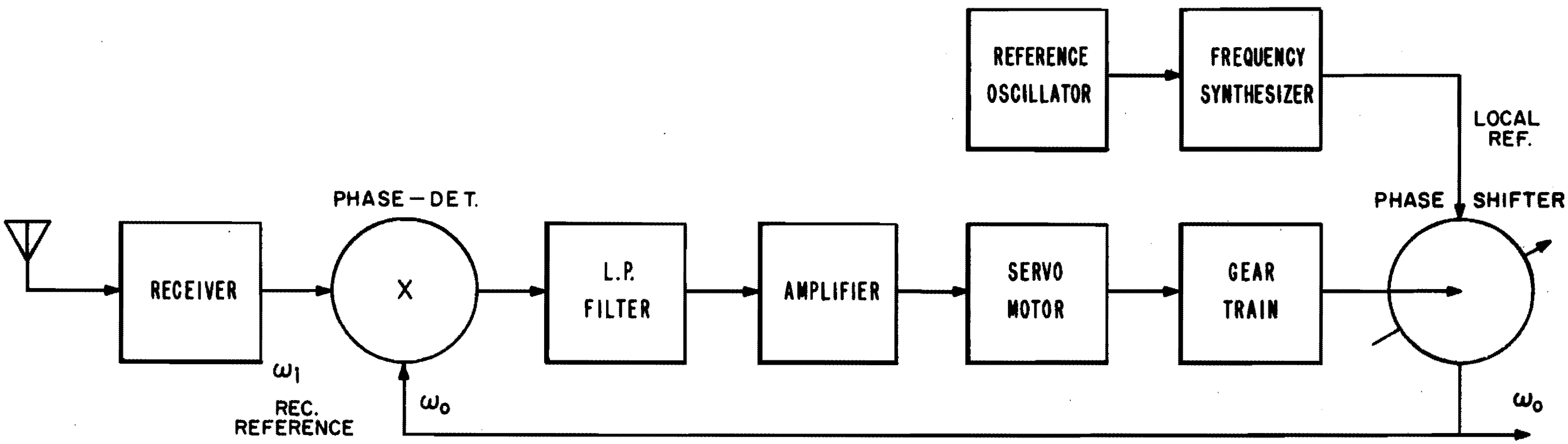

FIG. 9 DIAGRAM OF THE SYSTEM

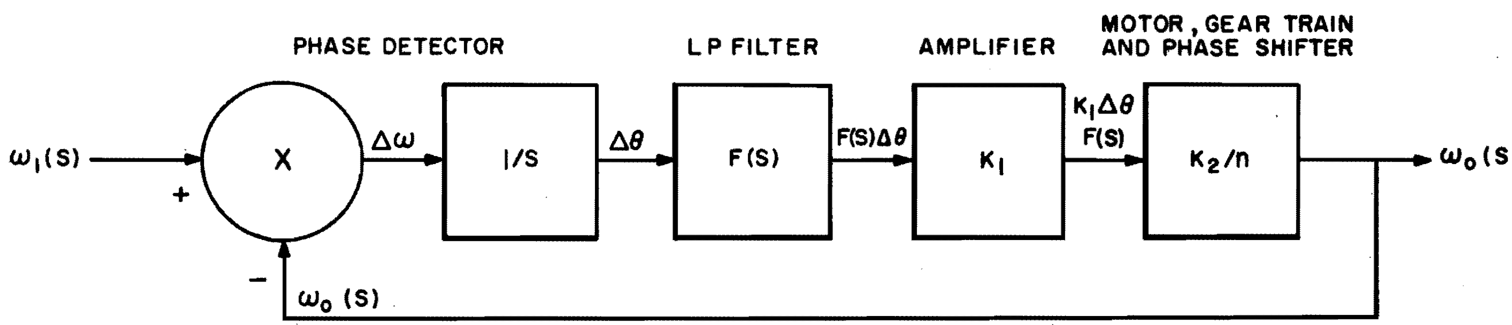

FIG. 10 DIAGRAM OF SYSTEM AS A SERVOSYSTEM

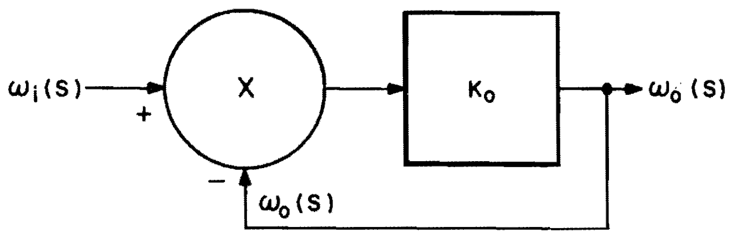

FIG. 11 SIMPLIFIED DIAGRAM

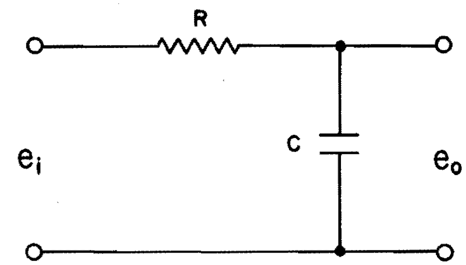

FIG. 12 RC FILTER

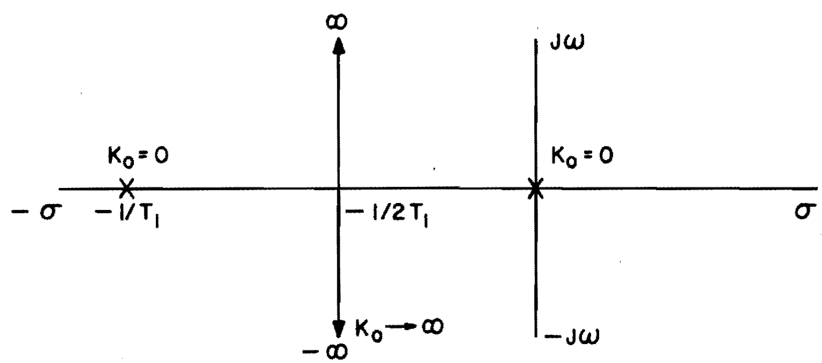

FIG. 13 ROOT LOCUS PLOT IN S PLANE

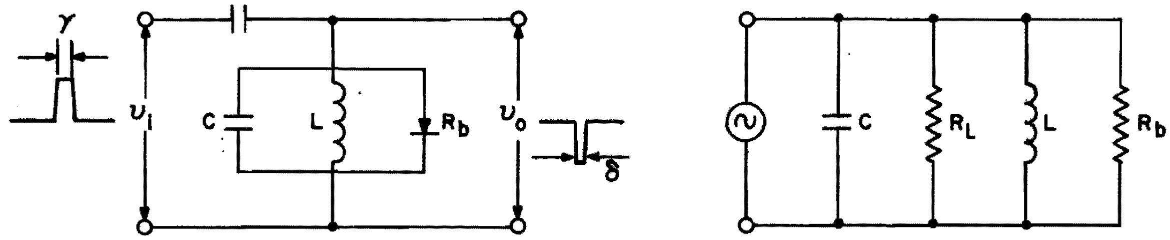

(a) CIRCUIT (b) EQUIVALENT CIRCUIT

FIG. 14 PULSE SHARPENING CIRCUIT

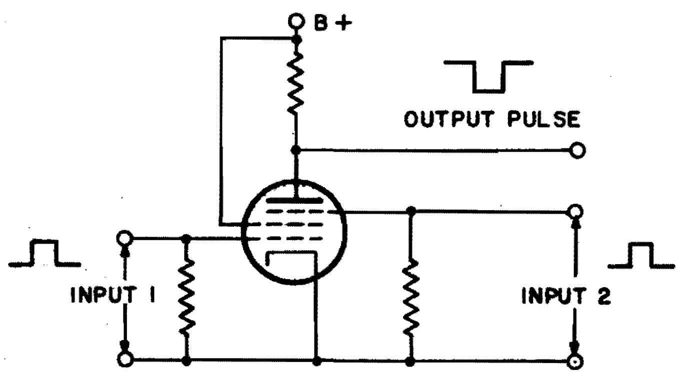

FIG. 15 PULSE COINCIDENCE CIRCUIT

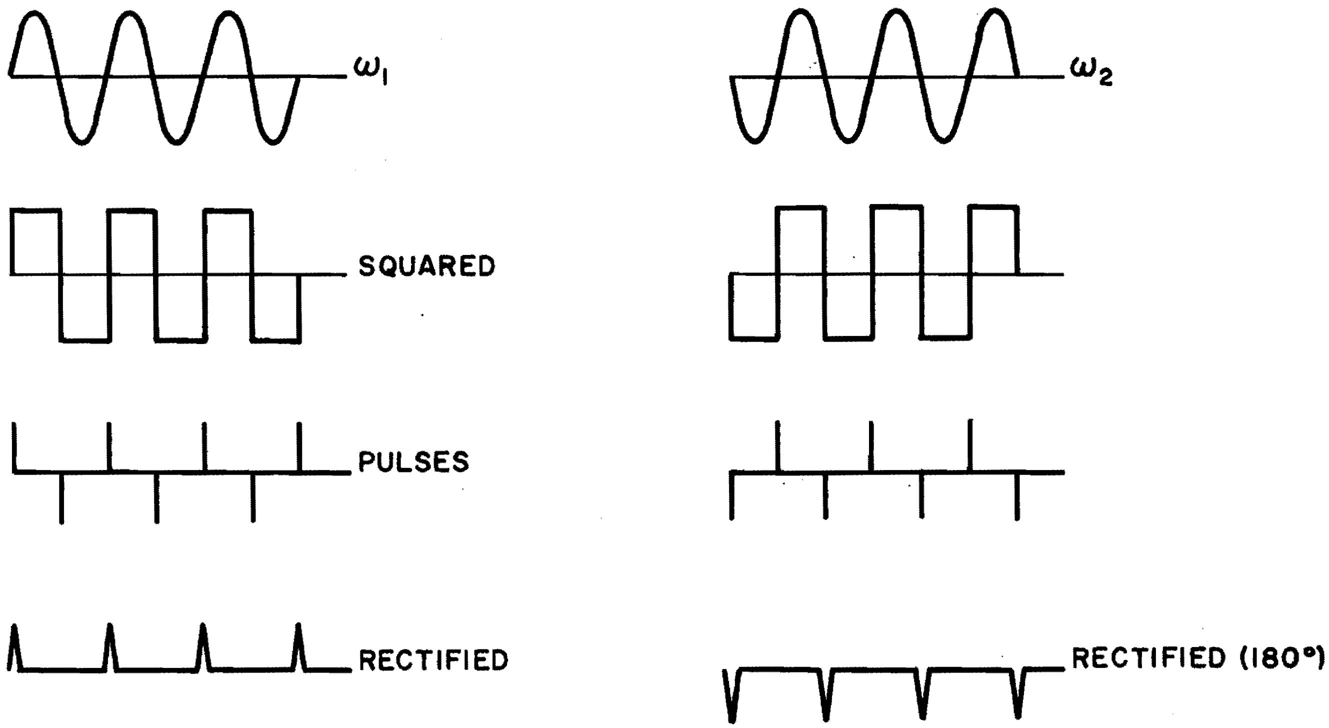

Fig. 16 WAVEFORMS

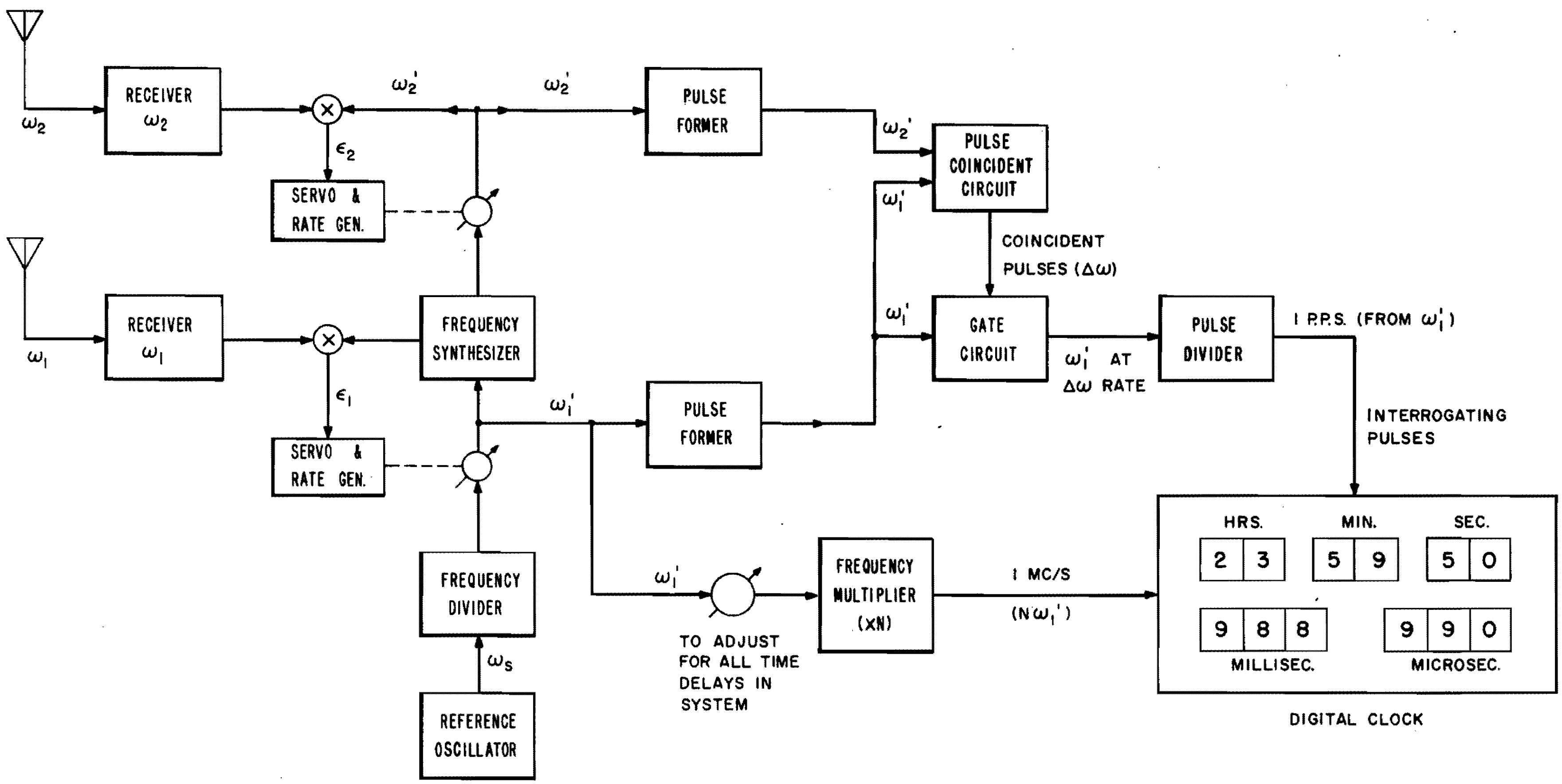

FIG. 17 20 KC DIGITAL CLOCK - USING SPACED CARRIERS

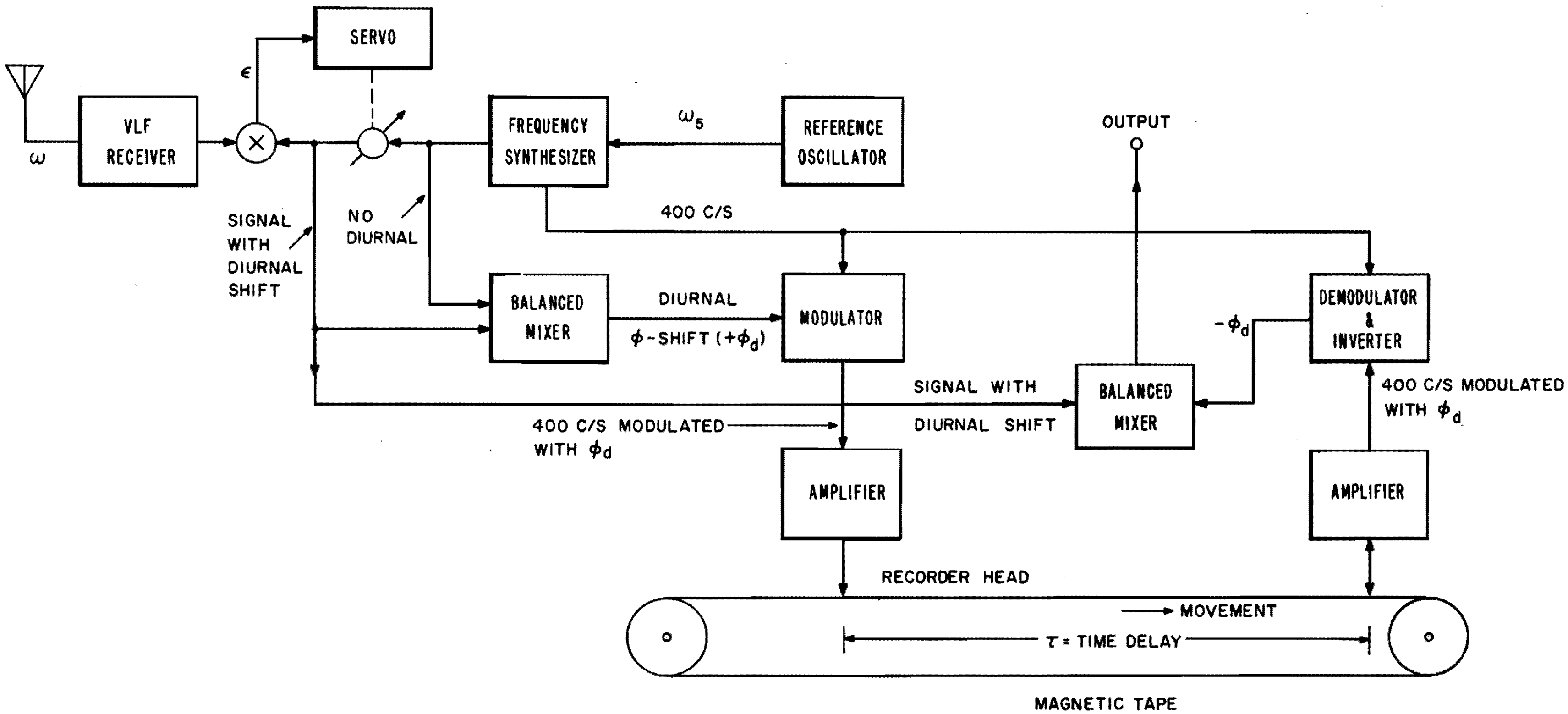

FIG. 18 VLF DIURNAL PHASE-SHIFT COMPENSATOR